

Reply to the first reviewer.

This manuscript evaluated eleven different parameterization methods in Tibetan Plateau using three ground stations. I don't see any errors as all eleven methods are well-established and have been extensively evaluated elsewhere else.

Reply: Thanks.

My questions are as follows.

Lines 115 -117: Zhu et al. (2017) evaluated 13 clear-sky and 10 all-sky DLR models based on hourly DLR measurements at 5 automatic meteorological stations. What are the differences between your work and Zhu's work in 2017?

Reply: Our major point is that clear-sky DLR parameterization may be seriously impacted by clear-sky data samples that are very likely contaminated by cloud residuals if human observations of cloud or hourly DLR measurements are used as the unique criteria in selecting data samples. Our result (Fig 3) clearly showed that clear-sky DLR in the previous studies was very likely overestimated by cloud residuals, which would significantly affect studies that take the clear-sky DLR estimation as their prior requirement, for example, cloud DLR forcing. Moreover, we studied the relationship between cloud base height and DLR that has never been investigated in the TP before. We consider these are our original contributions to our understanding of DLR parameterization in the TP. This research would be not possible if a comprehensive measurement project had not been performed. As one of important parts of a cooperated field campaign, the state-of-the-art pyranometer and pyrgeometer with ventilation and heating system are used to respectively measure downward shortwave and longwave radiation with 1-minute resolution, in addition, Lidar measurements provide much more information about clouds than before. To our best knowledge, installation of radiometers and Lidar side by side has never been performed, furthermore, 1-minute measurements are very rarely reported in the TP. These should be our novel aspects of experimental method, which indeed favors for our DLR parameterization study.

Lines 188 191: Can you use the actual SSA value, for example from any satellite product, instead of one mean value for three station? Surface albedo varies with time. Can you use any satellite product or measure it in situ?

Reply: There are few satellites providing aerosol SSA product except OMI. Given aerosol loading is very low, it is nearly impossible to retrieve precise SSA from satellite, therefore, we used a mean climatic value of SSA in study.

We did not measure surface albedo in TP and then used surface albedo observation results in same sites and periods from other researchers. Because our observations cover a short period, temporal variation of surface albedo is not likely a key issue in this study.

Reply to the second reviewer.

The manuscript evaluated and locally calibrated 11 clear-sky and 4 cloudy DLR parameterizations using high temporal resolution radiation measurements over TP in summer months. Three methods were combined to discriminate clear sky from clouds, which play an important role in improving the accuracy of parameterizations. The influence of CBH on DLR under overcast conditions was analyzed and a parameterization considering CBH was introduced. The topic is of sufficient interest to the communities of study on solar modelling and climate change. I recommend this paper for publication after revision.

Reply: We greatly appreciate the reviewer's opinions and revised the manuscript according to your valuable comments and suggestion.

Comments:

1. "W•m-2", "Wm-2", and "W/m2" appear in the manuscript and they should be unified.

Reply: We thoroughly revised the manuscript and unified them into "W·m⁻²".

2. Line32: Is the overestimation of clear-sky DLR found in one pervious study or some studies? The statement should be changed to "in one previous study" or "in previous studies".

Reply: Done, thanks.

3. Line 56: If "those remote regions" refer to some particular regions?

Reply: No, we just mean regions without surface observation. We corrected "those" into "some" in manuscript.

4. The abbreviation "T" refers to screen-level temperature in Line 64 and air temperature in Line 295. Different abbreviations should be used.

Reply: Thanks, we corrected this content in manuscript.

5. Line 97: Two predicate verbs appear in one sentence.

Reply: Thanks, we corrected this problem.

6. Line 105: Change "of highly significance" to "of high significance" or "highly significant".

Reply: Thanks, we change it to "of high significance".

7. Line 120: Change "root mean square" to "root mean square error".

Reply: Done, thanks.

8. Line 151: Change "make it having" to "make it have".

Reply: Done, thanks.

9. Line 157: If you want to express "side-by-side"?

Reply: Yes, thanks, we corrected the word into “side-by-side” in manuscript.

10. Line 161: What does “the dataset” refer to?

Reply: “the dataset” means all data we used in this article, we added explanation in the manuscript.

11. Line 187-188: The machine model of Cimel sunphotometer is usually expressed as “CE-318”.

Reply: Thanks, we changed “CIE-318” to “CE-318” in manuscript.

12. Line 188-189: Why did the authors adopt the same Angstrom wavelength exponent and Angstrom turbidity in NQ as that in AL? Please confirm the rationality. In addition, the rationality of adopting mean SSA in Lhasa should also be explain.

Reply: NQ and AL have similar altitude (4507 m ASL and 4287 m ASL) and climate (relatively dry) in three sites. Therefore, using Angstrom wavelength exponent and Angstrom turbidity data in AL rather than that in NC is rational.

Considering the extreme low aerosol loading in TP, we simplified the influence of aerosol on DSR_{cal} by using climatic values. Lhasa, which has long-period SSA observation, can provide relatively stable climatic value of SSA in TP. So we decided to use the mean SSA at Lhasa in this study.

Thanks for the suggestion, and we added this content in manuscript.

13. Line 189: Units of latitude and longitude should be added.

Reply: Thanks, we found that we mentioned the latitude, longitude and altitude (with units) of Lhasa in Line 164, so we deleted this content in Line 189.

14. Line 228: Change “an abruptly changes” to “an abrupt changes”.

Reply: Done, thanks.

15. Line 262: Change “Previous studies suggests” to “Previous studies suggest”.

Reply: Done, thanks.

16. Line 283-285: It is suggested to explain the bad performance of parameterization proposed by Swinbank (1963) and Idso and Jackson (1969).

Reply: We added this content, thanks for suggestion.

17. Line 371: References are needed.

Reply: Done, thanks.

18. Line 388-389: Change “introduce” to “introduction” and “significance” to “significant”.

Reply: Done, thanks.

1 **A revisit of parametrization of downward longwave radiation in**
2 **summer over the Tibetan Plateau based on high temporal resolution**
3 **measurements**

4 Mengqi Liu^{a,c}, Xiangdong Zheng^d, Jinqiang Zhang^{a,b,c} and Xiangao Xia^{a,b,c}

5 ^a LAGEO, Institute of Atmospheric Physics, Chinese Academy of Sciences, Beijing,
6 100029, China

7 ^b Collaborative Innovation Center on Forecast and Evaluation of Meteorological
8 Disasters, Nanjing University of Information Science & Technology, Nanjing 210044,
9 China

10 ^c College of Earth and Planetary Sciences, University of Chinese Academy of Sciences,
11 Beijing, 100049, China

12 ^d Chinese Academy of Meteorological Sciences, Chinese Meteorological Bureau,
13 Beijing, 100081, China

14

15

Abstract

16
17 The Tibetan Plateau (TP) is one of research hot spots in the climate change research
18 due to its unique geographical location and high altitude. Downward longwave
19 radiation (DLR), as a key component in the surface energy budget, is of practical
20 implications for radiation budget and climate change. A couple of attempts have been
21 made to parametrize DLR over the TP based on hourly or daily measurements and crude
22 clear sky discrimination methods. This study uses 1-minute shortwave and longwave
23 radiation measurements at three stations over TP to parameterize DLR during summer
24 months. Three independent methods are used to discriminate clear sky from clouds
25 based on 1-minute radiation and Lidar measurements. This guarantees strict selection
26 of clear sky samples that is fundamental for the parameterization of clear-sky DLR.
27 Eleven clear-sky and four cloudy DLR parameterizations are examined and locally
28 calibrated. Comparing to previous studies, DLR parameterizations here are shown be
29 characterized by smaller root mean square error (RMSE) and higher coefficient of
30 determination (R^2). Clear-sky DLR can be estimated from the best parametrization with
31 RMSE of $3.8 \text{ W}\cdot\text{m}^{-2}$ and $R^2 > 0.98$. Systematic overestimation of clear-sky DLR by the
32 locally calibrated parametrization in [one](#) previous study is found to be approximately
33 $25 \text{ W}\cdot\text{m}^{-2}$ (10%), which is very likely due to potential residual cloud contamination on
34 previous clear-sky DLR parametrization. Cloud-base height under overcast conditions
35 is shown to play an important role in cloudy DLR parameterization, which is considered
36 in the locally calibrated parameterization over the TP for the first time. Further studies
37 on DLR parameterization during nighttime and in seasons except summer are required
38 for our better understanding of DLR's role in climate change based on 1-minute high-
39 quality DLR measurements.

40

41

42 **1 Introduction**

43 The downward longwave radiation (DLR) at the Earth's surface is the largest
44 component of the surface energy budget, being nearly double the downward shortwave
45 radiation (DSR) (Kiehl and Trenberth, 1997). DLR has shown a remarkable increase
46 during the process of global warming (Stephens et al., 2012). This is closely related to
47 the fact that both a warming and moistening of the atmosphere (especially at the lower
48 atmosphere associated with the water vapor feedback) positively contribute to this
49 change. Understanding of complex spatiotemporal variation of DLR and its implication
50 is necessary for improving weather prediction, climate simulation as well as water
51 cycling modeling. Unfortunately, errors in DLR are considered substantially larger than
52 errors in any of the other components of surface energy balance, which is most likely
53 related to the lack of DLR measurements with high quality (Stephens et al., 2012).

54 The 2-sigma uncertainty of DLR measurement by using a well-calibrated and
55 maintained pyrgeometer is estimated to be 2.5% or $4 \text{ W} \cdot \text{m}^{-2}$ (Stoffel, 2005). However,
56 global-wide surface observations are very limited, especially in [some](#) remote regions.
57 On the other hand, it has been known for almost one century that clear-sky DLR is
58 determined by the bulk emissivity and effective temperature of the overlying
59 atmosphere (Ångström, 1918). Since these two quantities are not easily observed for a
60 vertical column of the atmosphere, clear-sky DLR is widely parameterized as a function
61 of surface air temperature and water vapor density, assuming that the clear sky radiates
62 toward the surface like a grey body at screen-level temperature. Dozens of
63 parameterization formulas of DLR have been developed in which clear-sky effective
64 emissivity (ϵ_c) is a function of the screen-level temperature (T) and water vapor pressure
65 (e) ([T and e have the same meaning and unit in following equations if not specified](#)), or
66 simply in the localized coefficients with given functions. Two formulas, i.e., an
67 exponential function (Idso, 1981) and a power law function (Brunt, 1932; Swinbank,
68 1963), have been widely used to depict the relationship of ϵ_c to T and e . The coefficients
69 of these functions are derived by a regression analysis of collocated measurements of
70 T , e and DLR. Most of these proposed parameterizations are empirical in nature and
71 only specific for definite atmospheric condition. An exception is that Brutsaert (1975)

72 developed a model based on the analytic solution of the Schwarzschild's equation for a
73 standard atmospheric lapse rates of T and e . Prata (1996) found that the precipitable
74 water content (w) was much better to represent the effective emissivity of the
75 atmosphere than e , which was loosely based on radiative transfer simulations. Dilley
76 and O'Brien (1998) adopted this scheme but tuned empirically their parameterization
77 using an accurate radiative transfer model. Since DLR is to some extent impacted by
78 water vapor and temperature profile (especially in case of existence of an inversion
79 layer) and diurnal variation of T , a new model with two more coefficients considering
80 these effects was developed (Dupont et al., 2008).

81 In the presence of clouds, total effective emissivity of the sky is remarkably
82 modulated by clouds. The existing clear-sky parameterization should be modified
83 according to the cloud fraction (CF) and other cloud parameters such as cloud base
84 height (CBH). CF is generally used to represent a fairly simple cloud modification
85 under cloudy conditions. Dozens of equations with cloudiness correction have been
86 developed and evaluated by DLR measurements across the world (Crawford and
87 Duchon, 1999; Niemela et al., 2001). CF can be obtained by trained human observers
88 (Iziomon et al., 2003) or derived from DSR (Crawford and Duchon, 1999) and DLR
89 measurements (Dürr and Philipona, 2004). High temporal resolution of DSR or DLR
90 measurements (for example, 1-minute) can also provide cloud type information
91 (Duchon and O'Malley, 1999), and thereby allow to consider potential effects of cloud
92 types on DLR (Orsini et al., 2002).

93 With an average altitude exceeding 4 km above the sea level (ASL), the Tibetan
94 Plateau (TP) exerts a huge influence on regional and global climate through mechanical
95 and thermal forcing because of its highest and most extensive highland in the world
96 (Duan and Wu, 2006). TP, compared to other high altitude regions and the poles, has
97 been relatively more sensitive to climate change. The most rapid warming rate over the
98 TP occurred in the latter half of the 20th century **was** likely associated with relatively
99 large increase in DLR. Duan and Wu (2006) indicated that increase in low level
100 nocturnal cloud amount and thereby DLR could partly explain the increase in the
101 minimum temperature, despite decrease in total cloud amount during the same period.

102 By using observed sensitivity of DLR to change in specific humidity for the Alps,
103 Rangwala et al. (2009) suggested that increase in water vapor appeared to be partly
104 responsible for the large warming over the TP. Since the coefficients of certain
105 empirical parameterizations and their performances showed spatiotemporal variations,
106 establishment of localized DLR parameterizations over the TP is of **high** significance.
107 Further studies on DLR, including its spatiotemporal variability, its parameterization as
108 well as its sensitivity to changes in atmospheric variables, would be expected to
109 improve our understanding of climate change over the TP (Wang and Dickinson, 2013).

110 DLR measurements from high quality radiometer with high temporal resolution
111 over the TP are quite scarce. To the best of our knowledge, there are very few
112 publications on DLR and its parameterization over the TP. Wang and Liang (2009)
113 evaluated clear-sky DLR parameterizations of Brunt (1932) and Brutsaert (1975) at 36
114 globally distributed sites, in which DLR data at two TP stations were used. Yang et al.
115 (2012) used hourly DLR data at 6 stations to study major characteristics of DLR and to
116 assess the all-sky parameterization of Crawford and Duchon (1999). Zhu et al. (2017)
117 evaluated 13 clear-sky and 10 all-sky DLR models based on hourly DLR measurements
118 at 5 automatic meteorological stations. The Kipp & Zonen CNR1 is composed of CM3
119 pyranometer and CG3 pyrgeometer that are used to measure DLR and DSR,
120 respectively. The CG3 is the second class radiometer according to the International
121 Organization for Standardization (ISO) classification. The root mean square **error** of
122 hourly DLR is less than $5 \text{ W}\cdot\text{m}^{-2}$ after field recalibration and window heating correction
123 (Michel et al., 2008). Note that human observations of cloud every 3-6 hours or hourly
124 DLR and DSR data are respectively used to determine clear sky and cloud cover in
125 these previous studies.

126 In order to further our understanding of DLR and DSR over the TP, measurements
127 of 1-minute DSR and DLR at 3 stations over the TP using state-of-the-art instruments
128 have been performed in summer months since 2011. These data provide us opportunity
129 to evaluate clear-sky DLR models and quantitatively assess cloud impacts on DLR.
130 This study makes progress in the following aspects as compared to previous studies: 1)
131 clear-sky discrimination and CF estimation are based on 1-minute DSR and DLR

132 measurements that are objective in nature; 2) misclassification of cloudiness into cloud-
133 free skies would be minimized by adopting strict cloud-screening procedures based on
134 1-minute DSR, DLR and Lidar measurements; 3) potential effects of CBH on DLR are
135 also investigated. Localized parameterizations of clear-sky and all-sky DLRs are finally
136 achieved, which would be expected to improve DLR estimations over the TP.

137

138 **2. Site, Instrument and Data**

139 Measurements of DLR and DSR conducted 1~4 months over the TP at three
140 stations (Table 1), including Nagqu (NQ, 92.04°E, 31.29°N, 4507 m ASL), Nyingchi
141 (NC, 94.2°E, 29.4°N, 2290 m ASL) and Ali (AL, 80°E, 32.5°N, 4287 m ASL) are used
142 for the DLR parameterization. DLR and DSR were respectively measured by CG4 and
143 CM21 radiometers (Kipp & Zonen, Delft, Netherlands). The sampling frequency is 1
144 Hz and the averages of the samples over 1-minute intervals are logged on a Campbell
145 Scientific CR23X datalogger. Simultaneous 1-minute averages of T and e are taken
146 from the automatic meteorological stations. With the aid of its specific material and
147 unique construction, CG4 is designed for the DLR measurement with high reliability
148 and accuracy. Window heating due to absorption of solar radiation in the window
149 material, the major error source of DLR measurement, is strongly suppressed by its
150 unique construction conducting away the absorbed heat very effectively. CM21 is a
151 high performance research grade pyranometer. Introduction of individually optimized
152 temperature compensation for CM21 makes it have much a smaller thermal offset than
153 CM3. The installation of the CG4 and CM21 on the Kipp & Zonen CV2 ventilation
154 unit prevents dew deposition on the window of the CG4 and the quartz dome of the
155 CM21. The radiometers are calibrated before and after field measurements to the
156 standards held by the China National Centre for Meteorological Metrology.

157 A Micropulse Lidar (MPL-4B, Sigma Space Corporation, United States) was
158 installed side-by-side with radiometers. The Nd:YLF laser of the MPL produces an
159 output power of 12 μ J at 532 nm. The repetition rate is 2500 Hz. The vertical resolution
160 of the MPL data is 30 m and the integration time of the measurements is 30s. The MPL
161 backscattering profiles are used to identify the cloud boundaries and derive the CBHs

162 (He et al., 2013). The dataset [used in this article](#) contains about 700 hours of coincident
163 DLR, DSR, Lidar and meteorological measurements.

164 DLR and DSR were also measured at Lhasa (91.1°E, 29.9°N, 3649 m ASL) during
165 summer in 2012 using the same instruments as those in other stations. Lhasa data are
166 mainly used for independent validation because of no Lidar data there.

167

168 **3. Methods**

169 **3.1 Clear-sky discrimination**

170 Clear skies should be discriminated from cloudy conditions before performing
171 DLR parametrization, which is achieved by the synthetical analysis of DSR, DLR, and
172 CBH from MPL.

173 Following the method initiated by Crawford and Duchon (1999), we calculate two
174 quantities reflecting DSR magnitude and variability based on 1-minute observed DSR
175 (DSR_{obs}) and calculated clear-sky DSR (DSR_{cal}) values. DSR_{cal} is calculated by the
176 model C of Iqbal (1983), in which direct and diffuse DSR are parametrized separately.
177 Direct DSR (DSR_{dir}) is calculated as follows.

$$178 \quad DSR_{dir} = S_0 \tau_r \tau_w \tau_o \tau_a \tau_g \quad (1)$$

179 where τ_r , τ_w , τ_o , τ_a and τ_g are transmittances due to Rayleigh scattering, water
180 vapor absorption, ozone absorption, aerosol extinction and absorption by uniformly
181 mixed gases O₂ and CO₂, respectively. Diffuse radiation is estimated as the sum of
182 Rayleigh and aerosol scattering as well as multiple reflectance. Total ozone column
183 (DU) is provided by Brewer spectrophotometer. w values (cm) are from Vaisala-92
184 radiosonde profiles in AL and Global Position System measurements in NC and NQ,
185 respectively. They are used to create linear regression relationship to collocated ground
186 level e (hPa) measurements, which is then used to estimate w from 1-minute
187 measurements of e . Ångström wavelength exponent and Ångström turbidity are from
188 [CE-318 sunphotometer observations in NC and AL](#), while in NQ we adopt the same
189 value as that in AL ([there are no sunphotometer observation in NQ and NQ has similar](#)
190 [altitude and aerosol background level with AL](#)). Climatic value of single scattering
191 albedo retrieved from [long- period CE-318 observation in Lhasa](#) is 0.90 (Che et al.,

192 2019), which is used in three stations (for high altitude and extreme low aerosol loading
193 in TP). Surface Albedo is 0.25 and 0.22 in AI and NQ according to in situ measurements
194 (Liang et al., 2012). In NC, it is 0.183 (Zhao et al., 2011).

195 DSR_{cal} values are first scaled to a constant value of 1400 W·m⁻² for each minute of
196 each day. We adopt this value according to Duchon and O'Malley (1998) and Long and
197 Ackerman (2000), which only favors for a clear presentation of the normalized and
198 observed DSR values in the same figure. Afterwards, DSR_{obs} values are scaled by
199 multiplying the same set of scale factors. Finally, the mean and standard deviation of
200 the scaled DSR in a 21-minute moving window (± 10 minute centered on the time of
201 interest) are used for cloud screening. Selection of the width of 21-minute is empirical
202 but a consequence of having a reasonable time span for estimating the mean and
203 variance (Duchon and O'Malley, 1999). Clear-sky DSR should satisfy three
204 requirements: 1) ratio of DSR_{obs} to DSR_{cal} is within 0.95 to 1.05; 2) difference between
205 scaled DSR_{obs} and DSR_{cal} is less than 20 W·m⁻²; and 3) standard deviation (δ) of scaled
206 DSR_{obs} in a 21-minute moving window is less than 20 W·m⁻².

207 Temporal variability of DLR is also used for cloud screening according to Marty
208 and Philipona (2000) and Sutter et al. (2004). Here, δ of scaled DLR (scaled to 500
209 W·m⁻²) in a 21-minute moving window is used for this purpose. Cloud-free sample is
210 determined if δ is less than 5 W·m⁻².

211 Since both DSR and DLR experience difficulties in detecting clouds in the portion
212 of the sky far away from the sun (Duchon and O'Malley, 1999) or high-altitude cirrus
213 clouds (Dupont et al., 2008), coincident MPL backscatter measurements are used to
214 strictly select clear-sky samples. There should be a cloud element somewhere in the sky
215 when MPL identifies cloud, it is thus required that no clouds are detected by MPL in a
216 21-minute moving window, otherwise it is defined as cloudy.

217 Given the fact that these methods are complementary to each other to some extent
218 (Orsini et al., 2002), we use the following strategy to guarantee a proper selection of
219 clear-sky samples. If DSR, DLR and MPL measurements at the time of interest
220 synchronously satisfy these specified clear-sky conditions, the sample is thought to be
221 taken under unambiguously cloud-free condition; on the contrary, the measurement are

222 made under unambiguously cloudy condition if any method suggests cloudy. Our
223 following clear-sky and cloudy DLR parameterizations are respectively based on
224 measurements under unambiguously cloud-free (8195 minutes) and cloudy conditions
225 (69318 minutes).

226 Fig. 1 shows an example of clear sky discrimination results based on our method.
227 DSR_{obs} presents a smooth temporal variation from sunrise to about 14:00 (LST), being
228 consistent with DSR_{clr} . Similarly, DLR also varies very smoothly during the same
229 period when 21-minute standard deviations of DLR are $< 5 \text{ W}\cdot\text{m}^{-2}$. Both facts suggest
230 sunny and cloudless skies. This inference is supported by MPL that suggests no cloud
231 detected overhead. Contrarily, an abrupt changes of 1-minute DSR_{obs} and DLR are
232 evident during 14:00~17:00 LST and we can see DSR_{obs} occasionally exceeds the
233 expected DSR_{clr} , indicating frequent occurrence of fair weather cumuli clouds. MPL
234 detect a persistent thin cloud layer at 4 km above ground, which agrees with DSR and
235 DLR measurements very well.

236

237 3.2 Cloud fraction estimation

238 Given synoptic cloud observations are very limited and temporally sparse, various
239 parameterizations using DSR or DLR data have been developed to estimate CF (e.g.,
240 Deardorff, 1978; Marty and Philipona, 2000; Dürr and Philipona, 2004; Long et al.,
241 2006; Long and Turner, 2008). Because of good agreement between clear-sky DSR_{obs}
242 and DSR_{cal} calculated by the Iqbal C calculations (Iqbal, 1983; Gubler et al., 2012),
243 with mean bias of $1.7 \text{ W}\cdot\text{m}^{-2}$ and root mean square error (RMSE) of $10.7 \text{ W}\cdot\text{m}^{-2}$ (not
244 shown), we use Deardorff (1978)'s method to calculate CF from DSR_{obs} and DSR_{cal} .
245 The method is based on a fairly simple cloud modification to DSR as follows.

$$246 \quad CF = 1 - \frac{DSR_{obs}}{DSR_{cal}} \quad (2)$$

247 CF (no unit) has values ranging from 0 to 1. To avoid the error caused by abrupt
248 DSR variation, 21-minute mean DSR value rather than its instantaneous measurements
249 are used here.

250

251 **4 Results**

252 4.1 Clear-sky DLR parameterization evaluation and localization

253 Eleven clear-sky DLR (DLR_{clr}) parameterizations (Table 2) are evaluated based
254 on 1-minute DLR measurements under unambiguously cloud-free conditions. To
255 compare the performance of these 11 models, RMSE and the coefficient of
256 determination (R^2) are shown by a Taylor diagram in Fig. 2(a). Relatively smaller
257 RMSE (generally $< 15 \text{ W}\cdot\text{m}^{-2}$) and larger R^2 (>0.95) are derived for the Brutsaert (1975);
258 Konzelmann (1994), Dilley and O'Brien (1998) and Prata (1996) models. This is likely
259 because these parameterizations were developed in cool and dry areas, for example, in
260 England (Brutsaert, 1975); in Greenland (Konzelmann, 1994) and dry desert region in
261 Australia (Prata, 1996). The climate in those areas is likely similar to that over the TP
262 to some extent, so those parameterizations are expected to perform well. The higher
263 RMSE ($>37 \text{ W}\cdot\text{m}^{-2}$) and the lower R^2 (~ 0.7) are derived for Swinbank (1963) and Idso
264 and Jackson (1969) models. This can be partly explained by the fact that only T is used
265 in these two methods. Previous studies suggest substantial uncertainty (RMSE >37.5
266 $\text{W}\cdot\text{m}^{-2}$ and $R^2 < 0.75$) if water vapor effect on DLR_{clr} is not accounted for (Duarte et al.,
267 2006). Since w is very low over the TP and thereby DLR is highly sensitive to variation
268 of w in that case, much more attention should be paid to water vapor effect on the
269 parameterization of DLR_{clr} .

270 The coefficients in eleven parameterizations (Table 2) were originally calibrated
271 and determined in different geographical locations; therefore, they may not be the
272 optimal values for the TP. Thus we take use of 1-minute clear-sky DLR samples to
273 locally calibrate the parameters of these parametrizations. We use 10-fold cross-
274 validation method to determine the parameters. This is a widely used method to estimate
275 the skill of a regression model on unseen data. It is expected to result in a less biased or
276 less optimistic estimate of the model skill than other methods, such as a simple train/test
277 split (James et al., 2013). All the data was randomly dividing into 10 groups of
278 approximately equal size, the coefficients are computed by using 9 groups as training
279 set, and the remaining 1 group is used as validation. This procedure is repeated 10 times
280 to get the representational value of coefficients (with the lowest test error).

281 The coefficient values derived from the non-linear least-squares fitting of the
 282 DLR_{clr} parameterizations (Table 2) over the TP are presented in Table 3. For each fitted
 283 parameterization, we calculated RMSE and R^2 and the results are shown in Fig. 2b.
 284 When using the parameterizations with the locally fitted parameters, the accuracy of
 285 the parameterization relative to the published values is obviously improved. Most
 286 RMSEs are $< 10 \text{ W} \cdot \text{m}^{-2}$ except the parameterization proposed by Swinbank (1963) and
 287 Idso and Jackson (1969) that still produce the worst results (with R^2 of 0.71 and RMSE
 288 of $15 \text{ W} \cdot \text{m}^{-2}$) even after the parameters are locally calibrated. **This is probably because**
 289 **e is not considered in these two methods.**

290 The Dilley and O'Brien (1998)'s parameterization, which is initially developed by
 291 considering the adaptation of climatological diversities, is expected to be able to fit the
 292 measurements in tropical, mid-latitude and Polar Regions. This expectation is verified
 293 by its wide deployment in DLR_{clr} estimations in different climate regimes and altitude
 294 levels, for example, in the tropical lowland (eastern Pará state, Brazil) and the mild
 295 mountain area (Boulder, the United States) (Marthews et al., 2012; Li et al., 2017).
 296 The present study confirms that Dilley and O'Brien (1998) is the best clear-sky
 297 parameterization over the TP. The locally calibrated equation is as follows.

$$298 \quad DLR_{clr} = -2.53 + 158.10 \times \left(\frac{T}{273.16}\right)^6 + 106.40 \times \left(\frac{46.50 \times e}{2.50 T}\right)^{\frac{1}{2}} \quad (3)$$

299 ~~Where T and e represent air temperature (K) and water vapor pressure (hPa),~~
 300 ~~respectively.~~ The RMSE and R^2 of Eq.(3) are $\sim 3.8 \text{ W} \cdot \text{m}^{-2}$ and > 0.98 respectively, which
 301 are substantially lower than those in previous studies over the TP, for example, the
 302 RMSE was $9.5 \text{ W} \cdot \text{m}^{-2}$ (Zhu et al., 2017). The Dilley and O'Brien (1998)'s
 303 parameterization was suggested to be the most reliable estimates of DLR_{clr} over the TP
 304 (Zhu et al., 2017). Note that the parameters here differ quite a lot from their values (Zhu
 305 et al., 2017), as shown in Eq. (4).

$$306 \quad DLR_{clr} = 30.00 + 157.00 \times \left(\frac{T}{273.16}\right)^6 + 97.93 \times \left(\frac{46.50 \times e}{2.50 T}\right)^{\frac{1}{2}} \quad (4)$$

307 Fig.3 compares instantaneous clear-sky DLR data from measurements against
 308 calculations by Eq. (3) of this study and by Eq. (4) from Zhu et al. (2017). The former
 309 performs very well as shown by an overwhelmingly large number of data points falling

310 along or overlapping the 1:1 line. By contrast, the latter overestimates DLR by $25 \text{ W}\cdot\text{m}^{-2}$
311 2 (10%). This difference is not very likely due to different DLR measurements used to
312 produce Eq. (3) and (4) giving the following considerations. First, this systematic
313 overestimation is much larger than the expected uncertainty of DLR measurements (2.5%
314 or $4 \text{ W}\cdot\text{m}^{-2}$) (Stoffel, 2005). More important, comparison of cloudy DLR
315 parameterizations between this study and Zhu et al. (2017) showed good agreement
316 (not shown). Note that only 1-hour CG3 DLR observations are used for clear sky
317 discrimination in Zhu et al. (2017). This method was shown to be very likely
318 contaminated by the thin high cloud (Sutter et al., 2004). This certainly would produce
319 an overestimation of clear sky DLR parameterization since larger DLRs are associated
320 with potential residual clouds relative to real clear-sky DLRs.

321

322 **4.2 Parameterization of cloudy-sky DLR**

323 Parameterizations of cloudy-sky DLR (DLR_{cld}) are based on estimated DLR_{clr}
324 coupled with the effect of cloudiness or cloud emissivity, which depends primarily on
325 CF as well as other cloud parameters, like CBH and cloud type (Arking, 1990; Viúdez-
326 Mora et al., 2015). Four parameterizations (Table 4), which modifies the bulk emissivity
327 depending on CF, are assessed and locally calibrated in this section.

328 DLR_{clr} is estimated according to Eq. (3). The fitted values of the coefficients (using
329 10-Fold Cross-Validation) of the four cloudy parameterizations are presented in Table
330 4. RMSE and R^2 of original and locally fitted parameterizations over the TP are
331 presented in Fig. 4.

332 Relative to clear-sky conditions, cloudy parameterizations using the given
333 parameters have higher error RMSE (generally exceeding $35 \text{ W}\cdot\text{m}^{-2}$) except that
334 developed by Jacobs (1978) (RMSE of $18 \text{ W}\cdot\text{m}^{-2}$). R^2 was generally smaller than 0.9.
335 RMSE values decrease significantly in Maykut and Church (1973) and Sugita and
336 Brutsaert (1993) as locally calibrated parameters are used. Relative smaller and almost
337 no RMSE improvements are found for the methods developed by Konzelmann (1994)
338 and Jacobs (1978).

339 Eq. (5) shows the best cloudy-sky parameterization over the TP by combining the

340 clear-sky parameterization of Dilley and O'Brien (1998) with the cloud modulation
341 correction scheme of Jacobs (1978).

$$342 \quad \text{DLR}_{\text{cld}} = (1 + 0.23 \times \text{CF}) \times \left(59.38 + 113.70 \times \left(\frac{T}{273.16} \right)^6 + 96.96 \times \left(\frac{46.50 \times \frac{e}{T}}{2.50} \right)^{\frac{1}{2}} \right) \quad (5)$$

343 RMSE and R^2 are $\sim 18 \text{ W} \cdot \text{m}^{-2}$ and ~ 0.89 respectively. RMSE here is close to $15 \text{ W} \cdot \text{m}^{-2}$
344 obtained in different altitude areas in Swiss (Gubler et al., 2012) and slightly lower than
345 $23 \text{ W} \cdot \text{m}^{-2}$ obtained in mountain area in Germany (Iziomon et al., 2003). Comparing to
346 previous studies over the TP (RMSE of $22 \text{ W} \cdot \text{m}^{-2}$ in Zhu et al., 2017), our cloudy model
347 produces better results.

348 In order to validate the newly developed DLR parameterizations, clear-sky and
349 cloudy-sky DLR parameterizations are validated against DLR measurements at Lhasa.
350 The results are shown in Fig. 5. Compared to the existed parameterizations, the Eq.(3)
351 and Eq.(5) produce the smallest bias (both less than $2 \text{ W} \cdot \text{m}^{-2}$) and RMSE (Eq.(3)'s is
352 less than $5 \text{ W} \cdot \text{m}^{-2}$ and Eq.(5)'s is less than $25 \text{ W} \cdot \text{m}^{-2}$). This independently demonstrates
353 the improved DLR parameterizations can be used in other stations over the TP.

354

355 **4.3 Effect of CBH on DLR under Overcast Conditions**

356 Since clouds behave approximately as a blackbody, the most relevant cloud
357 parameter (besides CF) to DLR under overcast skies (DLR_{ovc}) is CBH (Kato et al, 2011;
358 Viúdez-Mora et al., 2015): firstly, CBH defines the temperature of the lowest cloud
359 boundary, which through the Stefan-Boltzmann law drives the cloud emittance;
360 secondly, DLR emitted by the atmospheric layers above a cloud is totally absorbed by
361 the cloud itself (clouds are thick enough). Radiative transfer model simulation has
362 suggested that CBH under overcast conditions is an important modulator for DLR. The
363 cloud radiation effect (CRE), the difference between DLR_{obs} and DLR_{clr} , decreases with
364 increasing CBH at a rate of $4 \sim 12 \text{ W} \cdot \text{m}^{-2}$ that depends on climate profiles (Viúdez-Mora
365 et al., 2015). This indicates that overcast DLR parameterization would be improved if
366 CBH is considered.

367 A close relationship between CRE and CBH under overcast conditions over the TP
368 is presented in Fig 6. Compared to Viúdez-Mora (2015) results derived at Girona, Spain,

369 a mid-latitude site with low altitude, CRE over the TP is generally lower by 5~10 W·m⁻². This is likely because clouds over the TP with the same CBH as that at Girona have
370 2. This is likely because clouds over the TP with the same CBH as that at Girona have
371 relatively lower temperature, thereby producing lower radiative effect on DLR. CRE
372 generally decreases as CBH increases. The result agrees with the expectation since
373 CBH influence on DLR should decrease as CBH increases as a result of increasing
374 water vapor effects on DLR. According to Fig 6, CRE is about 70 W·m⁻² for clouds <
375 1 km and decreases to ~40 W·m⁻² for clouds at 3~4 km in TP. The decreasing rate of
376 CRE with CBH is estimated to be -9.8 W·m⁻²·km⁻¹ over the TP that agrees with model
377 simulations (Viúdez-Mora et al., 2015).

378 Since CBH effect on overcast DLR is apparent, we introduced a modified
379 parameterization to consider CBH effect on DLR under overcast conditions. A linear
380 correlation is firstly established based on the measured CBH and the ratio of observed
381 DLR (DLR_{ovc}^{obs}) and calculated DLR by Eq.(5) (DLR_{ovc}^{cal}) under overcast condition in Fig
382 6. Since we can see that DLR_{ovc}^{cal} is equal to DLR_{clr} times 1.23 (because CF is equal to
383 1 in Eq. 5), we derived a CBH corrected DLR_{ovc} parametrization as follows.

$$384 \quad DLR_{ovc} = 1.23 \times DLR_{clr} \times (1.07 - 0.046 \times CBH) \quad (6)$$

385 Where CBH has unit of km. The bias and RMSE of Eq. (6) between measurements
386 and calculations is -2.15 W·m⁻² and 19.79 W·m⁻², respectively, which are significantly
387 lower than that of Eq. (5) (10.3 W·m⁻² and 21.4 W·m⁻²) in overcast conditions. The
388 result indicates a remarkable improvement in the estimation of DLR under overcast
389 conditions by introducing CBH to the DLR parameterization; therefore, introduction of
390 such instruments as ceilometer to measure CBH is highly significant for studying
391 cloud's impacts on DLR.

392

393 **5 Discussion and conclusions**

394 The parameterization of clear-sky DLR requires a well-defined distinction
395 between clear-sky and cloudy-sky situations that commonly depends on human cloud
396 observations 4~6 times each day. Human observation is subjective in nature and its low
397 temporal resolution cannot resolve dramatic high-resolution variation of clouds.

398 Furthermore, synoptic human cloud observations show the tendency to stronger weight
399 to the horizon that DLR is not highly sensitive (Marty and Philipona, 2004). Clear sky
400 discrimination based on hourly DSR or DLR measurements also tends to be very
401 suspect of residual clouds due to their low temporal resolution. Parameterization of
402 clear-sky DLR based on these two methods is hence very likely biased as a consequence
403 of selection of cloud contaminated clear-sky measurements. This would result in biased
404 estimation of cloud DLR effect since it is the difference between clear-sky and
405 measured all-sky DLRs (Dupont et al., 2008).

406 Using 1-minute DSR and DLR at 3 stations over the TP, DLR parameterizations
407 are evaluated and localized parameterizations have been developed based on a
408 comprehensive cloud-screening method. We test the fitted parameterizations based on
409 independent DLR measurements at Lhasa. Potential CBH effect on overcast DLR is
410 experimentally determined. Major conclusions are as follows.

411 Among 11 clear-sky DLR parameterizations tested in this study, two methods
412 using only atmospheric temperature largely deviate from other parameterizations. The
413 best method suitable for TP is the parameterization developed by Dilley and O'Brien
414 (1998). DLR estimation can be improved by localization of these parameterizations.
415 Locally calibrated parameterization can produce clear sky DLR with RMSE of 3.8
416 $W \cdot m^{-2}$.

417 Overcast DLR is highly sensitive to CBH. The parameterization can be
418 substantially improved by consideration of CBH effect. The bias between empirically
419 parameterized calculations and measurements decreases from 10.3 to 1.3 $W \cdot m^{-2}$.

420 The focus of this study is on daytime DLR parameterization over the TP since DSR
421 is used in the cloud-screening method. Given a significant role of DLR played in the
422 surface energy budget during nighttime, it is highly desirable to perform further study
423 on the nighttime DLR parametrization. These results are based on summer DLR
424 measurements, so the conclusions here need to be further tested in other seasons,
425 especially in winter when an increasing tendency of DLR has been observed (Rangwala
426 et al., 2009). Further investigations on these issues are expected to shed new light on
427 how and why DLR has changed over the TP. Our results clearly showed substantial

428 CBH effect on overcast DLR, which would be considered in future when ceilometer is
429 widely used to measure CBH.

430

431 Acknowledgements: This work was supported by the Strategic Priority Research
432 Program of Chinese Academy of Sciences (XDA17010101), the National Key R&D
433 Program of China (2017YFA0603504), the National Natural Science Foundation of
434 China (91537213 and 91637107), the Special Fund for Meteorological Research in the
435 Public Interest (GYHY201106023), and the Science and Technological Innovation
436 Team Project of Chinese Academy of Meteorological Science (2013Z005) respectively
437 support the observations at AL, NQ and NC. We greatly appreciate Dr. Q. He for
438 providing the MPL Lidar measurement images and derived CBH data.

439 **References**

- 440 Ångström, A.: A study of the radiation of the atmosphere, Smithsonian Miscellaneous
441 Collection, 65, 1–159, 1915.
- 442 Arking, A.: The radiative effects of clouds and their impact on climate, *Bull. Am.*
443 *Meteorol. Soc.*, 72, 795-813, 10.1175/1520-
444 0477(1991)072<0795:Treoca>2.0.Co;2, 1991.
- 445 Brunt, D.: Notes on radiation in the atmosphere, *Q. J. Roy. Meteorol. Soc.*, 58, 389–
446 420, 1932.
- 447 Brutsaert, W.: On a derivable formula for long-wave radiation from clear skies, *Water*
448 *Resource Res.*, 11, 742–744, 1975.
- 449 Che, H., Xia, X., Zhao, H., Dubovik, O., Holben, B. N., Goloub, P., Cuevas-Agulló, E.,
450 Estelles, V., Wang, Y., Zhu, J., Qi, B., Gong, W., Yang, H., Zhang, R., Yang, L.,
451 Chen, J., Wang, H., Zheng, Y., Gui, K., Zhang, X., and Zhang, X.: Spatial
452 distribution of aerosol microphysical and optical properties and direct radiative
453 effect from the China Aerosol Remote Sensing Network, *Atmos. Chem. Phys.*
454 *Discuss.*, <https://doi.org/10.5194/acp-2019-405>, 2019.
- 455 Crawford, T. M., and Duchon, C. E.: An improved parameterization for estimating
456 effective atmospheric emissivity for use in calculating daytime downwelling
457 longwave radiation, *J. Appl. Meteorol.*, 38, 474–480, 1998.
- 458 Deardorff, J. W.: Efficient prediction of ground surface temperature and moisture, with
459 an inclusion of a layer of vegetation. *J. Geophys. Res.*, 83, 1889–1903, 1978.
- 460 Dilley, A. C., and O'Brien, D. M.: Estimating downward clear sky long-wave irradiance
461 at the surface from screen temperature and precipitable water, *Q. J. Roy. Meteorol.*
462 *Soc.*, 124a, 1391–1401, 1997.
- 463 Duan, A., and Wu, G.: Change of cloud amount and the climate warming on the Tibetan
464 Plateau, *Geophys. Res. Lett.*, 33, 10.1029/2006gl027946, 2006.
- 465 Duarte, H. F., Dias, N. L., and Maggionto, S. R.: Assessing daytime downward
466 longwave radiation estimates for clear and cloudy skies in Southern Brazil, *Agr.*
467 *Forest. Meteorol.*, 139, 171-181, 10.1016/j.agrformet.2006.06.008, 2006.
- 468 Duchon, C. E., and O'Malley, M. S.: Estimating cloud type from pyranometer
469 observations, *J. Appl. Meteorol.*, 38, 132-141, 1999.
- 470 Dupont, J. C., Haeffelin, M., Drobinski, P., and Besnard, T.: Parametric model to
471 estimate clear-sky longwave irradiance at the surface on the basis of vertical

472 distribution of humidity and temperature, *J. Geophys. Res.*, 113,
473 10.1029/2007jd009046, 2008.

474 Dürr, B., and Philipona, R.: Automatic cloud amount detection by surface longwave
475 downward radiation measurements, *J. Geophys. Res.*, 109, 9,
476 10.1029/2003jd004182, 2004.

477 Gubler, S., Gruber, S., and Purves, R. S.: Uncertainties of parameterized surface
478 downward clear-sky shortwave and all-sky longwave radiation, *Atmos. Chem.*
479 *Phys.*, 12, 5077-5098, 10.5194/acp-12-5077-2012, 2012.

480 He, Q. S., Li, C. C., Ma, J. Z., Wang, H. Q., Shi, G. M., Liang, Z. R., Luan, Q., Geng,
481 F. H., and Zhou, X. W.: The properties and formation of cirrus clouds over the
482 Tibetan Plateau based on summertime lidar measurements, *J. Atmos. Sci.*, 70, 901-
483 915, 10.1175/jas-d-12-0171.1, 2013.

484 Idso, S. B.: A set of equations for full spectrum and 8 to 14 μm and 10.5 to 12.5 μm
485 thermal radiation from cloudless skies, *Water Resource Res.*, 17, 295–304, 1981.

486 Iqbal, M.: *An Introduction to Solar Radiation*, Academic Press, Toronto, Canada, 1983.

487 Iziomon, M. G., Mayer, H., and Matzarakis, A.: Downward atmospheric longwave
488 irradiance under clear and cloudy skies: measurement and parameterization, *J.*
489 *Atmos. Solar-Terr. Phys.*, 65, 1107–1116, 2003.

490 Jacobs, J.D.: Radiation climate of Broughton Island, in: *Energy Budget Studies in*
491 *Relation to Fast-ice Breakup Processes in Davis Strait*, edited by Barry, R. G. and
492 Jacobs, J. D., *Inst. of Arctic and Alp. Res. Occas. Paper No. 26*. University of
493 Colorado, Boulder, pp. 105–120, 1978.

494 James, G., Witten, D., Hastie, T., and Tibshirani, R.: *An Introduction to Statistical*
495 *Learning: with Applications in R*, Springer-Verlag New York, USA, 2013.

496 Kato, S., Rose, F., Sun, S., Miller, W., Chen, Y., Rutan, D., Stephens, G., Loeb, N.,
497 Minnis, P., Wielicki, B., Winker, D., Charlock, T., Stackhouse Jr, P., Xu, K. M.,
498 and Collins, W.: Improvements of top-of-atmosphere and surface irradiance
499 computations with CALIPSO-, CloudSat-, and MODIS-derived cloud and aerosol
500 properties, *J. Geophys. Res.*, 116, D19209, 10.1029/2011JD016050, 2011.

501 Kiehl, J. T., and Trenberth, K. E.: Earth's annual global mean energy budget. *Bull. Am.*
502 *Meteorol. Soc.*, 78, 197-208, 1997.

503 Konzelmann, T., van de Wal, R. S. W., Greuell, W., Bintanja, R., Henneken, E. A. C.,
504 and Abe-Ouchi, A.: Parameterization of global and longwave incoming radiation
505 for the Greenland Ice Sheet, *Global Planet. Change*, 9, 143–164, 1994.

506 Li, M. Y., Jiang, Y. J., and Coimbra, C. F. M.: On the determination of atmospheric
507 longwave irradiance under all-sky conditions, *Sol. Energy.*, 144, 40-48,
508 10.1016/j.solener.2017.01.006, 2017.

509 Liang, H., Zhang, R. H., Liu, J. M., Sun, Z. A., and Cheng, X. H.: Estimation of hourly
510 solar radiation at the surface under cloudless conditions on the Tibetan Plateau
511 using a simple radiation model, *Adv. Atmos. Sci.*, 29, 675-689, 10.1007/s00376-
512 012-1157-1, 2012.

513 Long, C. N., Ackerman, T. P., Gaustad, K. L., and Cole, J. N. S.: Estimation of fractional
514 sky cover from broadband shortwave radiometer measurements, *J. Geophys. Res.*,
515 111, 11, 10.1029/2005jd006475, 2006.

516 Long, C. N., and Turner, D. D.: A method for continuous estimation of clear-sky
517 downwelling longwave radiative flux developed using ARM surface
518 measurements, *J. Geophys. Res.*, 113, 16, 10.1029/2008jd009936, 2008.

519 Marthews, T. R., Malhi, Y., and Iwata, H.: Calculating downward longwave radiation
520 under clear and cloudy conditions over a tropical lowland forest site: an evaluation
521 of model schemes for hourly data, *Theor. Appl. Climatol.*, 107, 461-477,
522 10.1007/s00704-011-0486-9, 2012.

523 Marty, C., and Philipona, R.: The Clear-Sky Index to separate clear-sky from cloudy-
524 sky situations in climate research, *Geophys. Res. Lett.*, 27, 2649-2652,
525 10.1029/2000gl011743, 2000.

526 Maykut, G. A., and Church P. E.: Radiation climate of Barrow, Alaska, 1962–1966, *J.*
527 *Appl. Meteorol.*, 12, 620–628, 1973.

528 Niemelä, S., Räisänen, P., and Savijärvi, H.: Comparison of surface radiative flux
529 parameterizations: Part I: Longwave radiation, *Atmos. Res.*, 58, 1–18, 2001a.

530 Orsini, A., Tomasi, C., Calzolari, F., Nardino, M., Cacciari, A., and Georgiadis, T.:
531 Cloud cover classification through simultaneous ground-based measurements of
532 solar and infrared radiation, *Atmos. Res.*, 61, 251-275, 10.1016/s0169-
533 8095(02)00003-0, 2002.

534 Prata, A. J.: A new long-wave formula for estimating downward clear-sky radiation at
535 the surface, *Q. J. Roy. Meteorol. Soc.*, 122, 1127–1151, 1996.

536 Rangwala, I., Miller, J. R., and Xu, M.: Warming in the Tibetan plateau: possible
537 influences of the changes in surface water vapor. *Geophys. Res. Lett.*, 36, 295-311,
538 2009.

539 Satterlund, D. R.: An improved equation for estimating longwave radiation from the

540 atmosphere, *Water Resource Res.*, 15, 1649–1650, 1979.

541 Stephens, G. L., Wild, M., Stackhouse, P. W., Jr., L'Ecuyer, T., Kato, S., and Henderson,
542 D. S.: The global character of the flux of downward longwave radiation, *J.*
543 *Climate.*, 25, 2329-2340, 10.1175/jcli-d-11-00262.1, 2012.

544 Stoffel, T.: Solar infrared radiation station (SIRS) handbook, Tech. Rep., ARM TR-025,
545 Atmos. Rad. Mea. Program, U.S. Dep. of Energy, Washington, D.C, 2005.

546 Sugita, M., and Brutsaert, W.: Cloud effect in the estimation of instantaneous downward
547 longwave radiation, *Water Resource Res.*, 29, 599-605, 10.1029/92wr02352, 1993.

548 Swinbank, W. C.: Long-wave radiation from clear skies, *Q. J. Roy. Meteor. Soc.*, 89,
549 330–348, 1963.

550 Viúdez-Mora, A., Costa-Surós, M., Calbó, J., and González, J. A.: Modeling
551 atmospheric longwave radiation at the surface during overcast skies: The role of
552 cloud base height, *J. Geophys. Res. Atmos.*, 120, 199–214, 10.1002/
553 2014JD022310, 2015.

554 Wang, K., and Liang, S.: Global atmospheric downward longwave radiation over land
555 surface under all-sky conditions from 1973 to 2008, *J. Geophys. Res.*, 114,
556 10.1029/2009jd011800, 2009.

557 Wang, K., and Dickinson, R. E.: Global atmospheric downward longwave radiation at
558 the surface from ground-based observations, satellite retrievals, and re-analyses,
559 *Reviews of Geophysics*, 51, 150-185, 10.1002/rog.20009, 2013.

560 Yang, K., Ding, B., Qin, J., Tang, W., Lu, N., and Lin, C.: Can aerosol loading explain
561 the solar dimming over the Tibetan Plateau? *Geophys. Res. Lett.*, 39,
562 10.1029/2012gl053733, 2012.

563 Zhao X., Peng B., Qin N., Wang W. (2011), Characteristics of Energy Transfer and
564 Micrometeorology in Surface Layer in Different Areas of Tibetan Plateau in
565 Summer (in Chinese), *Plateau and mountain Meteorology Research*,31(1), 6-11,
566 2011.

567 Zhu, M. L., Yao, T. D., Yang, W., Xu, B. Q., and Wang, X. J.: Evaluation of
568 parameterizations of incoming longwave radiation in the high-mountain region of
569 the Tibetan Plateau, *J. Appl. Meteorol. Climatol.*, 56, 833-848, 10.1175/jamc-d-
570 16-0189.1, 2017.

571

572

573 Table 1: Description of stations and measurements (magnitude and variability) in the

574

Tibetan Plateau

Site	Altitude (m ASL)	Period	T (°C)	e (hPa)	DLR ($W \cdot m^{-2}$)	Data Points
NQ	4507	2011.7.20- 2011.8.26	9.4 ± 8	7.4 ± 5	242.75 ± 40	52980
NC	2290	2014.6.7- 2014.7.31	16.8 ± 10	13.4 ± 4	368.25 ± 40	69609
AL	4279	2016.5.27- 2016.9.22	7.8 ± 4	4.8 ± 4	253.11 ± 50	86596

575

576

Table 2. 11 clear-sky DLR parameterizations and their specific conditions

Reference	Clear-Sky Parameterization	Conditions
Angstrom (1915)	$DLR_{clr} = \{0.83 - 0.18 \times 10^{-0.067e}\} \sigma T^4$	Alt.: 1650~3500 T: 283.15~303.15 e: 4~1
Brunt (1932)	$DLR_{clr} = (0.52 + 0.065\sqrt{e}) \sigma T^4$	Alt.: 6~3500 T: 269.15~303.15 e: 2.5~16
Swinbank (1963)	$DLR_{clr} = 5.31 \times 10^{-13} T^6$	Alt.: 2 T: 281.15~302.15 e: 8~30
Idso and Jackson (1969)	$DLR_{clr} = (1 - 0.261 \cdot \exp(-0.000777 \times (273 - T)^2)) \sigma T^4$	Alt.: 3, 331 T: 228.15~318.15
Brutsaert (1975)	$DLR_{clr} = 1.24 \left(\frac{e}{T}\right)^{\frac{1}{7}} \sigma T^4$	Alt.: 6~3500 T: 269.15~313.15 e: 2.5~16
Satterlund (1979)	$DLR_{clr} = 1.08 \left(1 - \exp\left(-e^{\frac{T}{2016}}\right)\right) \sigma T^4$	Alt.: 594 T: 236.15~309.15 e: 0~18hPa
Idso (1981)	$DLR_{clr} = \left(0.7 + 5.95 \times 10^{-5} \times e \times \exp\left(\frac{1500}{T}\right)\right) \sigma T^4$	Alt.: 331 T: 258.15~278.15 e: 2~6
Konzelmann (1994)	$DLR_{clr} = \left(0.23 + 0.443 \left(\frac{e}{T}\right)^{\frac{1}{8}}\right) \sigma T^4$	Alt.: 340~3230 T: 257.15~279.15 e: 1.5~5.5
Prata (1996)	$DLR_{clr} = (1 - (1 + 46.5 \frac{e}{T}) \times \exp(-(1.2 + 3 \times 46.5 \frac{e}{T})^{0.5})) \sigma T^4$	Not specified
Dilley and O'Brien (1998)	$DLR_{clr} = 59.38 + 113.7 \left(\frac{T}{273.16}\right)^6 + 96.96 \sqrt{46.5 \frac{e}{T} / 2.5}$	Not specified
Iziomon (2001)	$DLR_{clr} = \left(1 - 0.43 \exp\left(-\frac{11.5e}{T}\right)\right) \sigma T^4$	Alt.: 1489 $\bar{T} = 277.55 \bar{e} = 7.4$

578 *Where Alt. is the altitude above sea level, and its unit is (m ASL), e is screen-level water vapor

579 pressure in hPa and T represents surface temperature in K

580

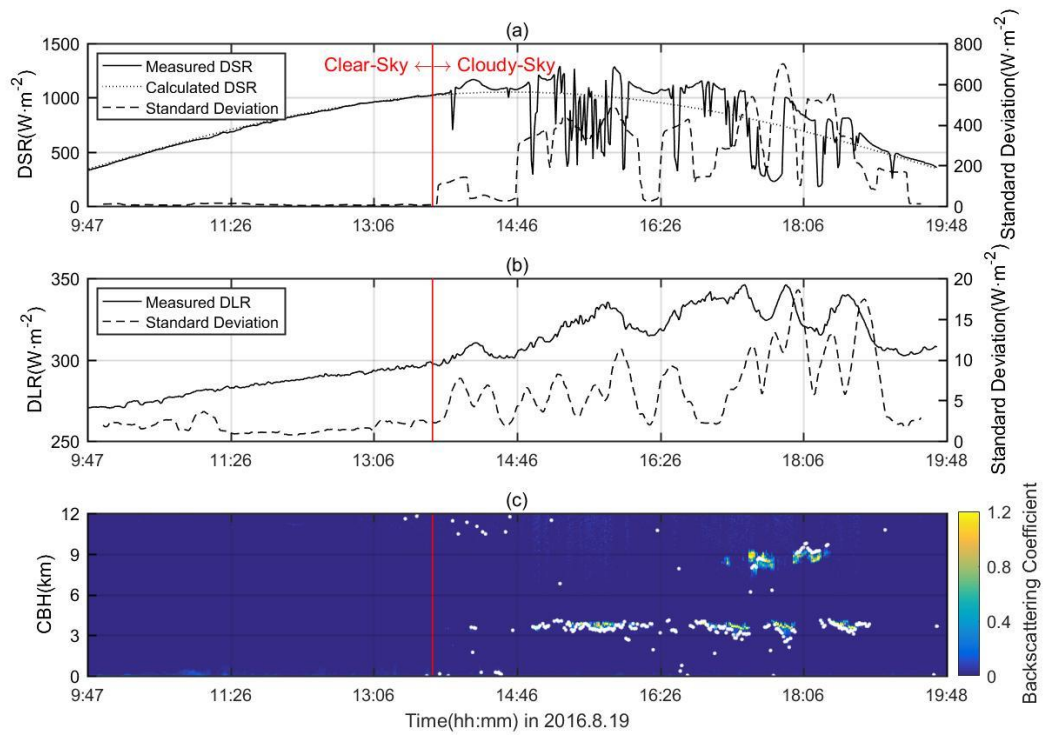
581

Table 3. Locally fitted clear-sky DLR parameterizations in TP

Reference	Locally fitted Clear-Sky Parameterization
Angstrom(1915)	$DLR_{clr} = \{0.8 - 0.19 \times 10^{-0.068e}\} \sigma T^4$
Brunt(1932)	$DLR_{clr} = (0.56 + 0.07\sqrt{e}) \sigma T^4$
Swinbank(1963)	$DLR_{clr} = 4.7 \times 10^{-13} T^6$
Idso & Jackson(1969)	$DLR_{clr} = (1 - 0.36 \cdot \exp(-0.00065 \times (273 - T)^2)) \sigma T^4$
Brutsaert(1975)	$DLR_{clr} = 1.03 \left(\frac{e}{T}\right)^{0.09} \sigma T^4$
Satterlun (1979)	$DLR_{clr} = \left(1 - \exp\left(-e^{\frac{T}{2016}}\right)\right) \sigma T^4$
Idso(1981)	$DLR_{clr} = \left(0.63 + 7.5 \times 10^{-5} \times e \times \exp\left(\frac{1500}{T}\right)\right) \sigma T^4$
Konzelmann(1994)	$DLR_{clr} = \left(0.23 + 0.45 \left(\frac{e}{T}\right)^{0.13}\right) \sigma T^4$
Prata(1996)	$DLR_{clr} = (1 - (1 + 46.5 \frac{e}{T}) \times \exp(-(1 + 3 \times 46.5 \frac{e}{T})^{0.5})) \sigma T^4$
Dilley and O'Brien(1998)	$DLR_{clr} = -2.54 + 158.1 \left(\frac{T}{273.16}\right)^6 + 106.4 \sqrt{46.5 \frac{e}{T} / 2.5}$
Iziomon(2001)	$DLR_{clr} = \left(1 - 0.38 \exp\left(-\frac{14.52e}{T}\right)\right) \sigma T^4$

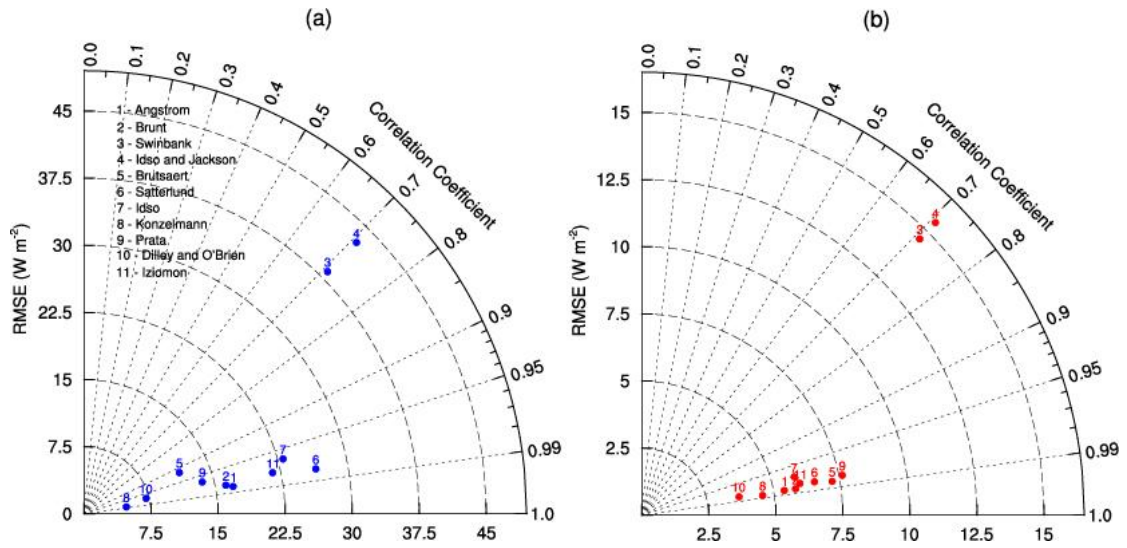
Table 4. 4 Ordinary and locally fitted cloudy-sky DLR parameterizations

Reference	DLR _{cl} Parameterization	Ordinary Parameters	Locally Fitted Parameters
Maykut(1973)	$(a + b \times CF^c)\sigma T^4$	a=0.7855 b=0.000312 c=2.75	a=0.85 b=0.01 c=3
Jacobs(1978)	$(1 + a \times CF)DLR_{clr}$	a=0.26	a=0.23
Sugita(1993)	$(1 + a \times CF^b)DLR_{clr}$	a=0.0496 b=2.45	a=0.2 b=1.3
Konzelmann(1994)	$(1 - CF^a)DLR_{clr} + b \times CF^a\sigma T^4$	a=4 b=0.95	a=3.5 b=1



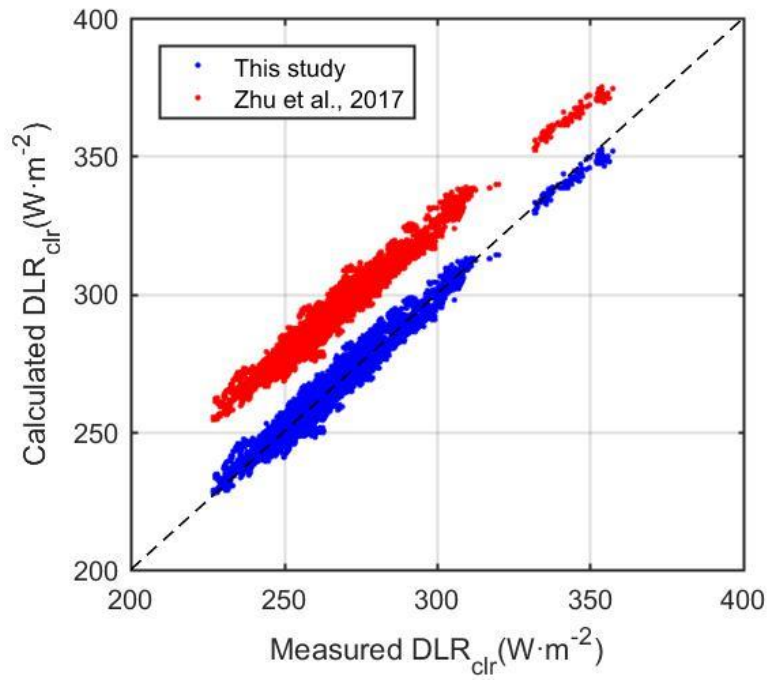
588

589 Fig. 1. Time series of data sample on 2016.8.19 transited from clear-sky to cloudy-sky: (a)
 590 measured (black line) and calculated (dotted black line) downward shortwave radiation and its 21-
 591 min standard deviation (grey line), (b) measured downward longwave radiation and 21-min standard
 592 deviation and (c) MPL backscattering coefficient and the cloud base height.



593
 594
 595
 596

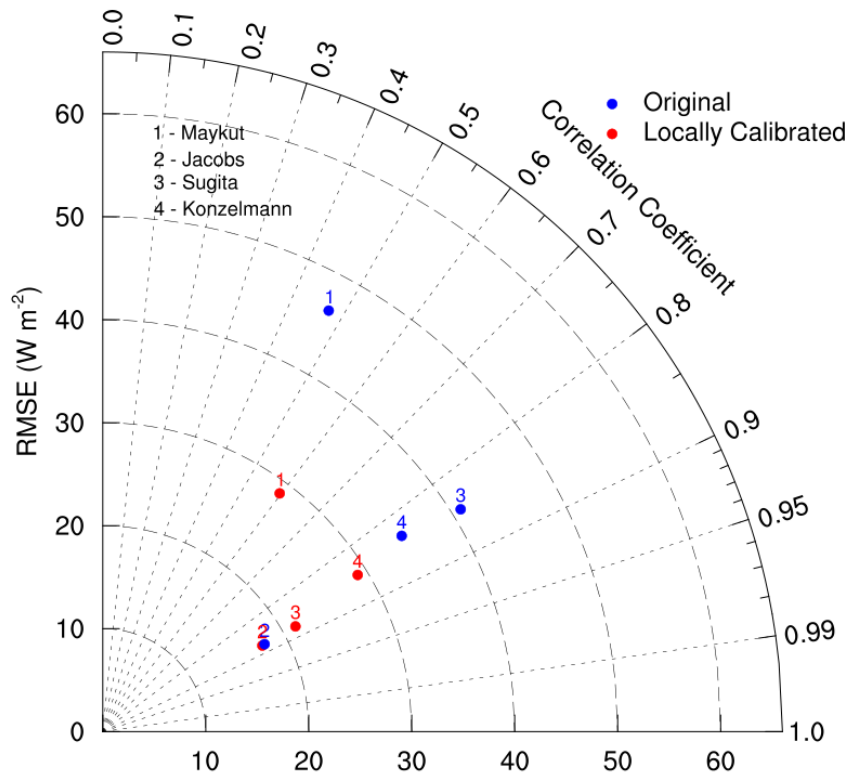
Fig. 2. RMSE and R^2 for the clear-sky DLR parameterizations using original (a) and locally calibrated (b) coefficients.



598

599 Fig. 3. Scatter plots of measured clear-sky DLR data from as a function of calculations
600 by the Eq.(3) this study (blue dots) and the Eq.(4) by Zhu et al. (2017) (red dots). The
601 dash black line is the 1:1 line.

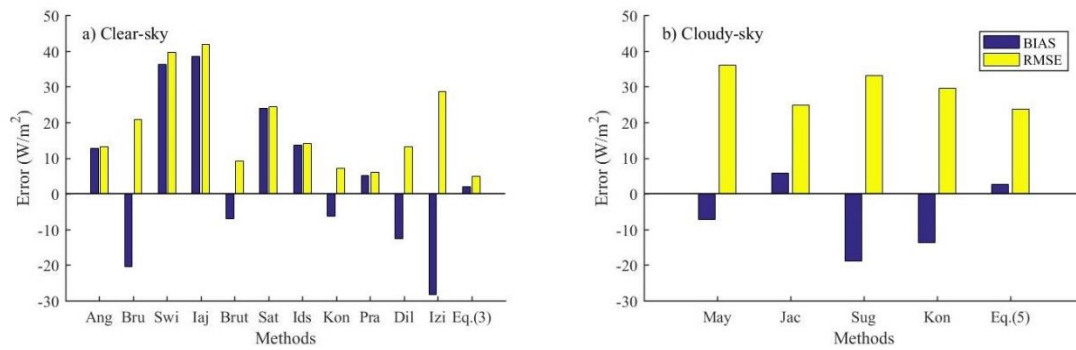
602



603

604 Fig. 4. RMSE and R^2 for the cloudy-sky DLR (DLR_{clD}) parameterizations using the
 605 original (blue) and locally calibrated (red) coefficient.

606

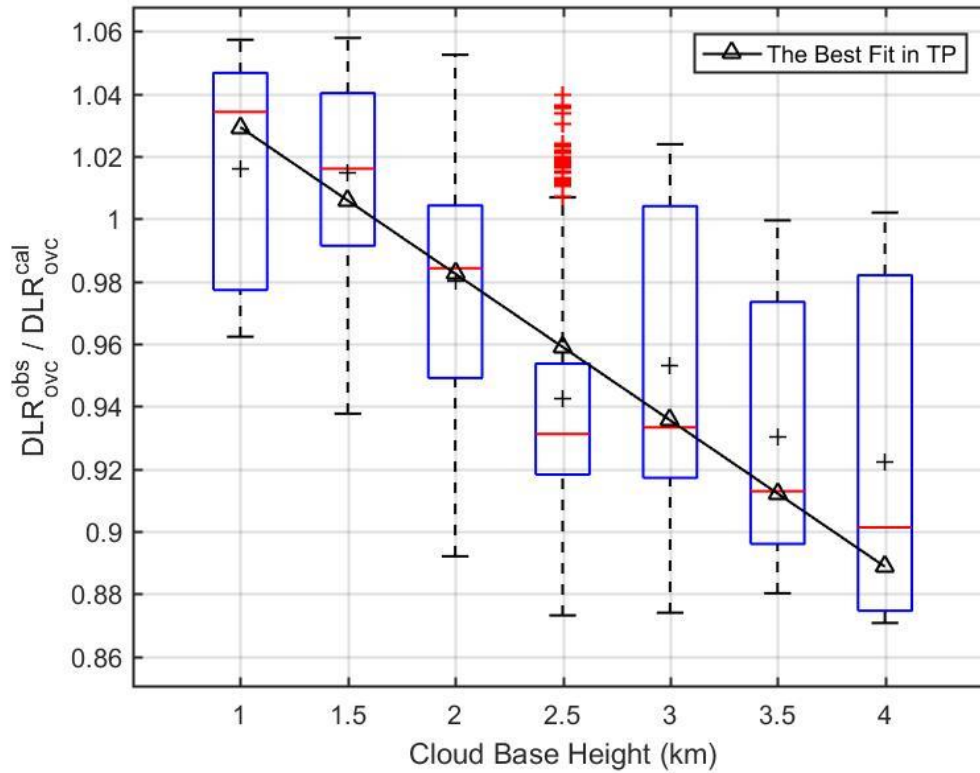


607

608 Fig. 5. BIAS and RMSE for the LDR parameterizations using (a) the published clear-sky
 609 and Eq.(3), and (b) cloudy-sky parameterizations and Eq.(5).

610

611



613

614 Fig. 6. Distributions of the ratio of observed DLR and calculated DLR by Eq.(5) under
 615 overcast condition against measured cloud base height are represented by box plot (the
 616 blue box indicates the 25th and 75th percentiles, the whiskers indicate 5th and 95th
 617 percentiles, the red middle line is the median, the black plus sign is the mean). The
 618 black triangle line is the fitting line.

619

